Integrating CFD and piloted simulation to quantify ship-helicopter operating limits

D. M. Roper, I. Owen, G. D. Padfield
Department of Engineering
The University of Liverpool
Liverpool, UK

S. J. Hodge
Flight Simulation Department
BAE Systems
Warton Aerodrome
Preston, UK

ABSTRACT

This paper describes a study which has been concerned with numerical predictions of the airwakes resulting from two simplified ship geometries: the internationally agreed Simple Frigate Shape, SFS1, and its successor, SFS2. Extensive steady-state simulations have been carried out for a wide range of wind conditions using Fluent, a commercially available Computational Fluid Dynamics (CFD) code. The CFD predictions have been partially validated against wind tunnel data produced by the National Research Council of Canada (NRC) and have shown good agreement. The resulting airwake velocity components have been exported from Fluent, interpolated onto suitable grids and attached to the FLIGHTLAB flight-simulation environment as look-up tables; piloted flight trials were then carried out using the Liverpool full-motion simulator. The pilot workload and helicopter control margins resulting from a range of wind-over-deck conditions have been used to develop the Ship-Helicopter Operating Limits (SHOL) for a Lynx-like helicopter and the SFS2. The workload was compared to the pilot's experiences on a similar aircraft and a Type 23 Frigate and the simulated SHOL compared with SHOLs derived from sea trials. The results are very encouraging and open up further the long awaited prospect of such simulations being used in the future to reduce at-sea trials, and to provide a safe environment for pilot training.

1.0 INTRODUCTION

The turbulent airwake produced by the flow of air over a ship has been the subject of much research in recent years[1-12]. A ship's airwake is dependent on many factors including the geometry of the ship, the strength and direction of the natural wind and free-stream turbulence, the sea condition and the motion of the ship in the seaway. This highly unsteady flowfield is further modified during ship-borne rotorcraft operations when the downwash from the helicopter's main rotor interacts with the airwake during launch and recovery manoeuvres, resulting in a fully coupled helicopter–ship dynamic interface. Furthermore, different helicopter and ship combinations will interact in different ways depending on the prevailing conditions[13-19]. When the helicopter is immersed in the ship's airwake, pilot workload is high and helicopter control margins are much reduced. In some circumstances, under the influence of strong winds and high levels of turbulence, workload can become unacceptably high and the pilot will be unable to achieve consistently accurate landings, thus compromising flight safety[3,10,20-26]. This situation is avoided in fleet service by operating the aircraft and ship within the boundaries specified by the Ship-Helicopter Operating Limits (SHOLs).

SHOLs define the safe boundaries of operation for a particular helicopter–ship combination in terms of maximum allowable wind speed and direction relative to the ship. In the UK, SHOLs are

Paper No. 3051. Received on 6 January 2006, accepted 27 April 2006.

https://doi.org/10.1017/S0001924000001329 Published online by Cambridge University Press

derived through a process known as First-of-Class Flight Trials (FOCFTs) carried out at sea. Typically, 3-5 weeks of sea trials are required to develop a SHOL for one helicopter/ship combination[27]. For example, the most recent set of FOCFTs to clear the Apache AH1 Attack helicopter to operate from the deck of the Royal Navy's helicopter carrier HMS *Ocean*, involved around 600 landings under a variety of different conditions[28]. During FOCFTs test pilots will repeatedly perform launch and recovery evolutions to the deck of the ship, beginning with relatively benign conditions and gradually progressing to more severe conditions until a limit is reached where the test pilot considers that the task would demand undue levels of skill and workload from an 'average' fleet pilot. The process is then repeated at every available wind condition and sea-state, at several different helicopter All-Up Mass (AUM) cases and also for night operations. This is both costly and time-consuming in terms of ship time and flying-hours. If suitable conditions are not encountered during the flight trials, then a limited SHOL envelope will be defined requiring expansion through further trials or read-across from other data sources, in order to meet operational requirements. Moreover, the process is risky, since the objective of the trial is to determine the limits of safe operation, through the identification of conditions at which maximum pilot workload or degradation in helicopter flying qualities occurs.

The prospect of using modelling and simulation to augment or even replace traditional at-sea testing is therefore an attractive one. The benefits of achieving high fidelity simulation of the helicopter-ship dynamic interface include reduced costs and the availability of a safe, controllable and repeatable environment, where any wind condition can be presented to the pilot an unlimited number of times. A high-fidelity dynamic interface simulation could be used to improve the design of future helicopters and ships, predict or expand SHOL envelopes for future and existing assets, and to train pilots. However, before modelling and simulation can be used with confidence for this application there are many technical challenges that must first be overcome. Foremost amongst these challenges is accurate modelling and real-time simulation of the airwake around the ship in order to induce representative levels of pilot workload in the simulator. Whilst a full treatment of the ship's airwake would require the unsteady flow around the hangar coupled with the helicopter rotor downwash to be solved in real time, an initial model can be developed by spatially mapping the topology of the air flow around the ship using numerical modelling techniques.

The study reported in this paper has primarily been concerned with the airwake resulting from two simplified ship geometries under a full range of wind conditions using CFD simulations. The ship geometries were defined by The Technical Co-operation Programme (TTCP)[4,7,29] for comparative experimental and CFD studies and are known as the Simple Frigate Shape (SFS1) and its successor (SFS2), (Fig. 1). TTCP has research partners in the UK, Canada, Australia and the USA with a common interest in modelling and simulation of the helicopter-ship dynamic interface. Extensive CFD modelling of these simplified geometries has given some insight into the nature of the airwake encountered by helicopters operating from frigates. This CFD data was integrated into The University of Liverpool's full-motion flight simulator. Deck landing trials were then carried out by a former Royal Navy test pilot flying a Lynx-like helicopter, resulting in the development of a typical SHOL for the SFS2/helicopter interface.

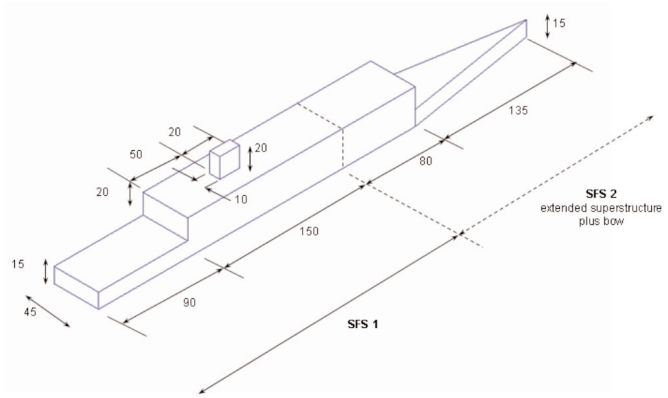


Figure 1. The SFS1 and SFS2 geometry (extended and pointed bow) All dimensions in feet.

2.0 AIRWAKE CFD

2.1 CFD details

In this study the commercial code Fluent was used to model the airwakes produced by the SFS1 and SFS2 for a wide range of relative wind directions. As the airwake changes considerably with wind azimuth, it is necessary to model each desired angle separately. However, the large Reynolds numbers associated with the ship size and free-stream wind velocities result in flows that can be considered to be Reynolds number independent[30]. Assuming Reynolds number and Wind-Over-Deck (WOD) independence[5,9] all numerical simulations were made for a free-stream inlet condition of $20ms^{-1}$ (about 40kt), and the wind strength was varied by scaling the solution velocity components within the range 10 to $50ms^{-1}$. A pressure outlet was defined in the domain and no-slip conditions applied to all surfaces of the simple frigate shapes, thereby enabling boundary layer growth. The sea, however, was modelled as a frictionless surface in order to eliminate ambiguous sea boundary layer issues. This was also appropriate because the available experimental data for the SFS1 was obtained from a model raised from the floor of the wind tunnel, and suction was used to reduce boundary layer effects for SFS2. All other boundaries (the side horizons and sky) were modelled as frictionless.

A number of different mesh topologies were developed, from hexagonal throughout to tetrahedral throughout, plus hybrid grids. Due to the complex flows over the ship for all wind directions, the grid could never be completely aligned with the flow, hence second order discretization for pressure was used, regardless of grid structure. The SIMPLEC algorithm was employed for pressure-velocity coupling and the higher order QUICK scheme for momentum and turbulence. Viscous, turbulent flow was modelled and the standard k-ω and realisable k-ε (two-equation) turbulence models were used and compared. More rigorous turbulence models are available, such as the Reynolds Stress (seven-equation) model, but these are computationally more expensive and the pursuit of grid-independence by solution-based adaption was given a higher priority within the constraints of available computing power and time. The $rk\varepsilon$ model gave slightly improved results in two test cases but the improvement was not significant. For the SFS1, wind angles encountered in the forward hemisphere relative to the ship were considered at 10° intervals, i.e. from –90° to +90°, while for the SFS2 a full range of wind angles from 0° to 360° were considered at 15° intervals. Winds from the port side of the ship are named Red winds, whilst those from the starboard side are named Green winds, in keeping with maritime terminology. Due to symmetry in both the SFS1 and SFS2, it was only necessary to perform CFD calculations on one side of the ship for each wind angle: the resulting flowfield was then reflected about the ship centreline. However, the resulting pairs of airwakes did provide different scenarios for piloted flight simulation, since the landing was always attempted from the port side of the ship, so the encountered airwake in each case was not the same.

https://doi.org/10.1017/S0001924000001329 Published online by Cambridge University Press

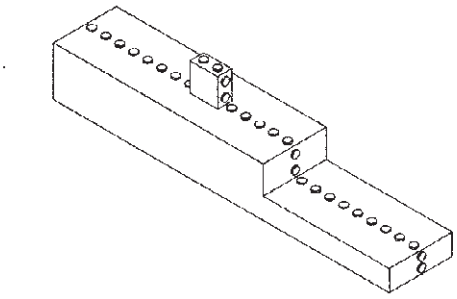


Figure 2. Example of pressure taps on the SFS1
Line 1 (ship longitudinal centreline).

2.2 CFD Validation

Validation of the CFD results was against experimental data provided by the National Research Council of Canada (NRC) for SFS1 and SFS2[27,29,31]. For the SFS1, experiments were conducted on a 1/60th scale model in a 2m × 3m low-speed wind tunnel. A raised turntable provided different yaw angles in a uniform free-stream velocity where flow visualisation and surface pressure coefficients were obtained. For the SFS2, a 1/100th scale model was used together with a turntable incorporating suction for boundary layer reduction. Hot wire anemometry was used to obtain *u,v* and *u,w* velocity components at points in the flow close to the ship, particularly over the flight deck.

The study was initially concerned with the airwakes resulting from different WOD conditions for the SFS1. For steady flow, wind angles were simulated for 1-5° inclusive, and for 10-90° in steps of 10°. The detailed flowfields for the SFS1 will not be given here since the more realistic SFS2 geometry has superseded SFS1.

Validation for the SFS1 was achieved by comparing pressure coefficients (*Cp*) measured at surface pressure taps on the frigate surface[29] with the equivalent *Cp* values calculated using CFD. For example, one set of pressure taps was aligned with the longitudinal centreline of the SFS1 as shown in Fig. 2, and Figs 3 and 4 show how the experimental and CFD centreline values compare for two different wind angles — ahead wind 0° (Fig. 3) and Red 30° (Fig. 4).

At 0 deg, the agreement is reasonably good, although it is poorest in areas of separation and reattachment around the 'bow' and the funnel. A more rigorous turbulence model may be justified in these regions. Good general agreement was also obtained for Red 30°, with the largest deviations again found in regions where separation and re-attachment occurred. The solutions were checked for grid-independence, and it is likely that further improvement would need to be from the choice of turbulence model.

The second phase of this investigation moved forwards with the introduction of a more realistic frigate geometry, the SFS2 (Fig. 1). A comprehensive steady-state CFD investigation was carried out for a range of wind directions with the aim of creating a database of SFS2 airwakes for implementation in the simulator.

Each initial solution was progressively adapted using velocity gradients as a parameter, followed by grid quality checks such as adjacent cell volume changes. Adaptions were carried out after each converged solution until grid independence was achieved or approached. Experimental data from NRC was available for the SFS2 with 0° head wind and with Green 45° wind, in the form of normalised velocity components along specified maps of in-line

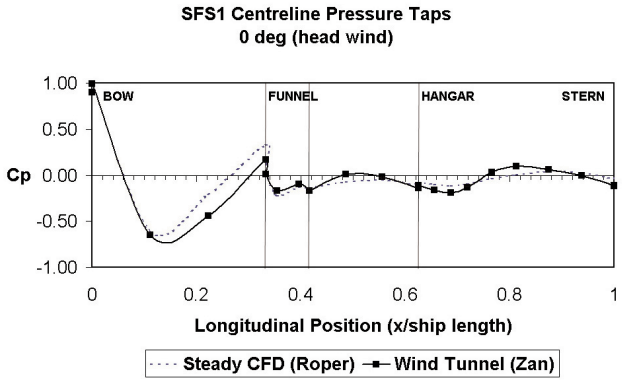


Figure 3. SFS1 *Cp* (CFD and exp)
Head Wind (0°), line 1 (ship longitudinal centreline).

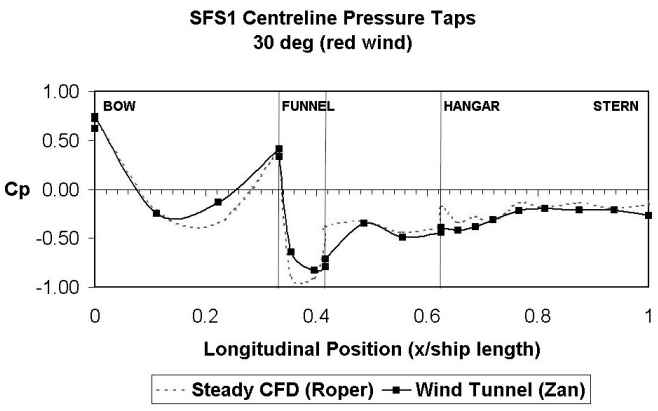


Figure 4. SFS1 *Cp* (CFD and exp)
Red 30 , line 1 (ship longitudinal centreline).

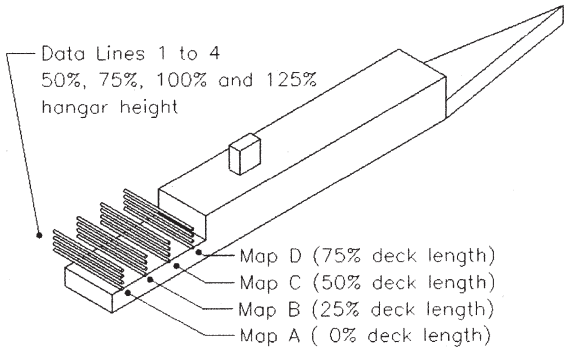


Figure 5. SFS2 experimental and CFD
data point maps for 45° validation.

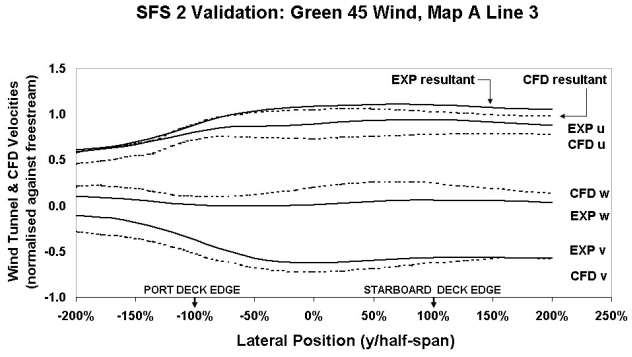


Figure 6. SFS2 Green 45° wind: map A, line 3
CFD and experimental *u, v, w* velocity components and resultant velocity.

https://doi.org/10.1017/S0001924000001329 Published online by Cambridge University Press

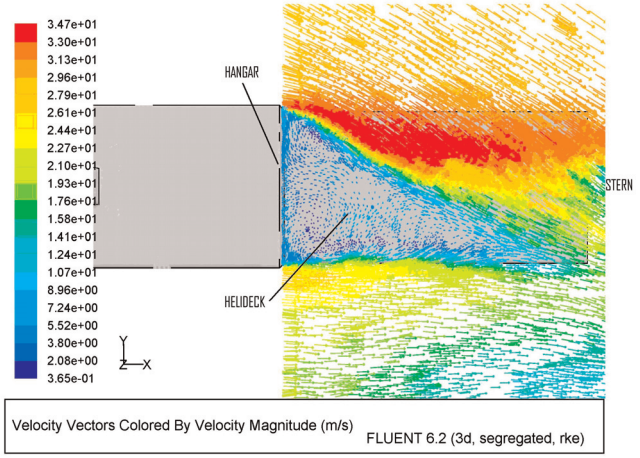


Figure 7. SFS2 Green 45° velocity vectors
Mid-hangar height over landing deck

points. For example, referring to Figure 5, for 45°, Maps A to D represent sections at 0%, 25%, 50% and 75% deck length, with lines increasing in height from the deck.

All available experimental data was compared to the CFD solutions; one example, which was typical of the agreement found, is shown in Figure 6. This compares the three computed velocity components and resultant velocity with the corresponding measured values along Map A, Line 3 for a Green 45° wind. This line is at the back of the flight deck and level with the top of the hangar. The overall agreement between the CFD and the NRC data for both SFS1 and SFS2 was considered to be reasonably good and gave confidence that the computed flowfield for the steady airwake was suitable for use in the flight simulator.

Having produced satisfactory CFD solutions, each airwake was visualised using velocity and pressure contour plots and velocity vector plots. Figure 7 is a plan view over the landing region towards the ship stern. This is just one illustration which shows the velocity field at mid-hangar height around the flight deck with the wind coming from 45° to starboard. The complex flowfield and steep velocity gradients are clearly seen and it is these features that contribute to the pilot workload as the helicopter rotor translates through this airflow.

3.0 DEVELOPING THE SIMULATION

3.1 Experimental facilities

The main research and simulation tool used by the Flight Science and Technology Research Group at the University of Liverpool is HELIFLIGHT, a PC-based high-fidelity re-configurable flight simulator (Fig. 8). The main features of the simulator include a six degree of freedom motion platform, four-axis programmable control loaders, and a three-channel collimated visual display for forward view, plus two chin windows. For this series of trials a basic frigate model was introduced to the visual scene with flight deck and hangar dimensions scaled to match the geometry of the SFS2. The position of the frigate model remained fixed during the trials and all tests were performed in simulated daylight conditions over the open ocean. The simulator cockpit is equipped with three conventional pilot inceptors: cyclic, collective and rudder pedals. Overall transport delays between pilot inceptor inputs and motion base/visual system response are estimated to be less than 50ms. A full description of the University of Liverpool simulator can be found in the literature[32,33].

3.2 Helicopter flight dynamics model

The helicopter model used for the simulation trials was constructed in FLIGHTLAB, an advanced multi-body dynamics modelling and simulation environment which allows complete rotorcraft simulations to be constructed from a set of modular components. For the present study, a single main rotor generic helicopter model was constructed, representative of a Lynx-type helicopter. A blade element representation of the main rotor was used, including dynamic inflow to model the delay in the reaction of the air mass in the vicinity of the main rotor to changes in rotor forces and moments. The tail rotor was modelled using a Bailey disc model and aerodynamic models of the fuselage and empennage were also included. A basic Stability and Control Augmentation System (SCAS) was modelled and engaged throughout the trials. An undercarriage model was included to provide deck reaction cues on touchdown. The airwake velocities were applied to the helicopter model at five points along each of the main rotor blades, at the main and tail rotor hubs and at the aerodynamic centres of the fuselage and empennage (Fig. 9).

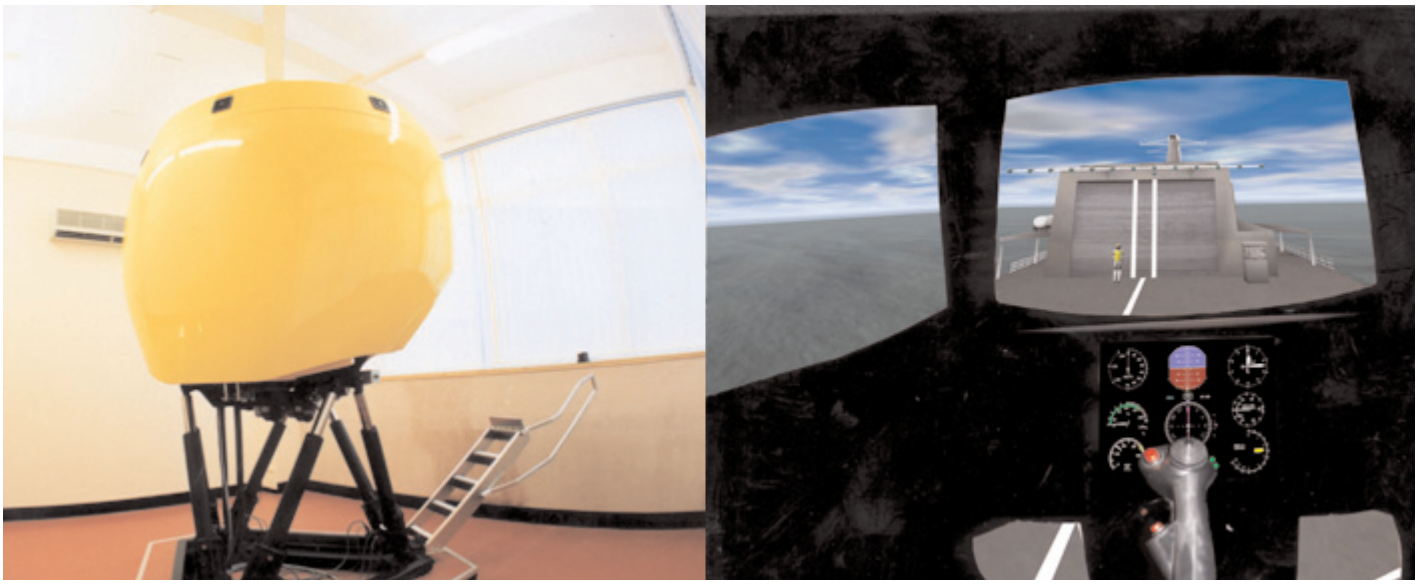


Figure 8. The Liverpool full-motion flight simulator (HELIFLIGHT).

https://doi.org/10.1017/S0001924000001329 Published online by Cambridge University Press

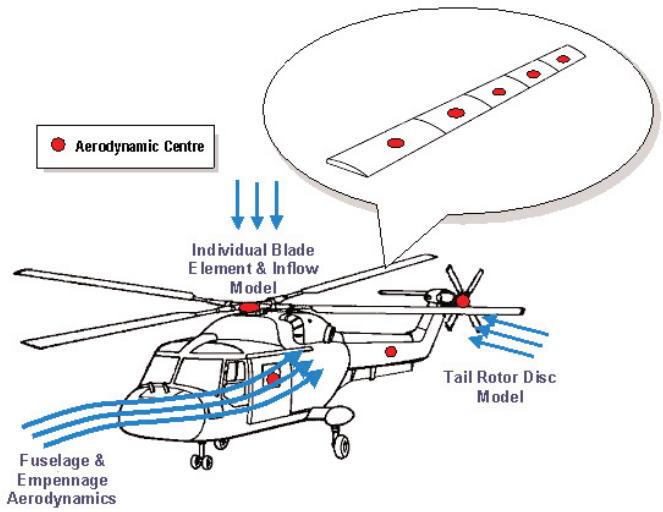


Figure 9. Helicopter and airwake model integration

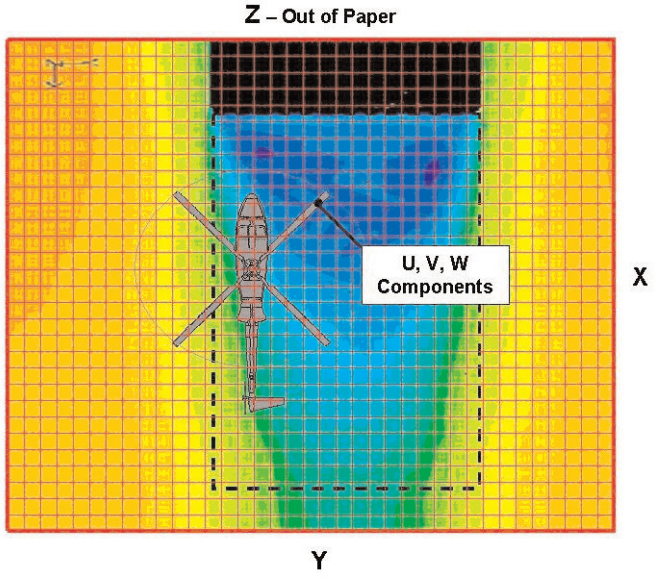


Figure 10. Calculating the local airwake components.

The generic Lynx FLIGHTLAB model can currently be described as a medium fidelity model. Handling qualities parameters are reasonably well predicted by this standard of modelling[34]. However, the aerodynamic interactions between the main-rotor wake and tail rotor, which often causes a loss of tail rotor effectiveness in starboard quartering winds (Green 60°) due to the main rotor wake becoming entrained in the tail rotor, is not completely captured by medium fidelity models[34-36]. This is not unusual for real-time simulation, since faithful reproduction of this effect requires a full implementation of an aeroelastic blade-element main rotor and vortex wake model integrated with a blade element tail rotor model. Further investigation into the use of off-line data, from non-realtime main rotor–tail rotor interaction models, to enhance the fidelity of real-time ship-helicopter simulations is required for more accurate prediction of pedal control margins during the deck landing task[36].

3.3 Ship airwake model

The ship airwake model was used to model the effects of the three-dimensional velocity flowfield around the ship on the helicopter flight dynamics and flying qualities. In order to simplify the situation it was assumed that the presence of the helicopter and its rotor downwash does not modify the flowfield encountered by the rotor. Therefore, the airwake model can be derived from the results of steady-state CFD simulations of the SFS2 geometry described in the previous section. These three-dimensional steady-state CFD simulations resulted in large quantities of data, including the longitudinal, lateral and vertical velocity components of the flowfield around the SFS2, sampled at each point or node, on an unstructured grid. In this irregular grid format the data is unsuitable for direct implementation into look-up table format for real-time simulation. Therefore, the velocity components of the flowfield (u, v and w) and the spatial distribution of the nodes (X, Y and Z) were imported into MATLAB for further processing. This processing involved reducing the size of the solution domain to cover only the area that the helicopter will operate in, then re-interpolating the remaining data onto a structured grid. The resulting domain covered an area extending approximately 190m (625ft) aft of the SFS2 hangar face, 45m (150ft) in height and 60m (200ft) either side of the ship centreline. The resolution of the grid spacing in the structured grid became coarser as distance from the SFS2 increased, but was set to 1m in the vicinity of the hangar face and flight deck. The resulting data was written in the FLIGHTLAB TAB-file format and loaded directly into the FLIGHTLAB helicopter model at runtime. Figure 10 shows a plan view of the structured grid for a head-on wind with the helicopter model in place. During each real-time simulation run the spatial location of the helicopter's main and tail rotor hubs and fuselage, empennage and rotor blade element aerodynamic centres are computed relative to the ship. The resulting offsets (X, Y and Z) are then used to extract the local u, v and w velocity components of the airwake at each point using a three-dimensional interpolation scheme.

In order to develop a SHOL for the SFS2 and candidate rotorcraft, it was necessary to develop several airwake look-up tables for each possible wind direction around the ship in 15 degree steps. The topology of the flow changes considerably when the direction of the wind is changed, so there is no alternative other than to perform a new CFD simulation for each wind direction of interest. Fortunately, since the SFS2 is exactly symmetrical the airwake flowfields from the Red side of the SHOL plane can be reflected and used for the Green side of the SHOL (e.g. Red 30° flowfield can also be used for Green 30°); this of course is not true of most real-life ships where, for example, placement of weapons and other deck equipment can make the vessel non-symmetric. Note that it does not follow that the pilot will experience identical effects using the 'reflected' airwakes. In the simulation trials the pilot was instructed to always approach from the port side of the ship.

The effect of the airwake is to increase pilot workload. This is illustrated in Fig. 11, which compares lateral cyclic control activity in a 40 knot head wind, with and without the airwake being present. Movements of all the controls, in all wind conditions were recorded during the flight tests.

4.0 TRIALS CONDUCT

4.1 Deck landing mission task elements

A Mission Task Element (MTE) is an element of a mission that can be treated as a handling qualities task. A mission can be constructed from a contiguous sequence of MTEs, each with distinct start and end conditions and defined goals in terms of flight and mission performance.

https://doi.org/10.1017/S0001924000001329 Published online by Cambridge University Press

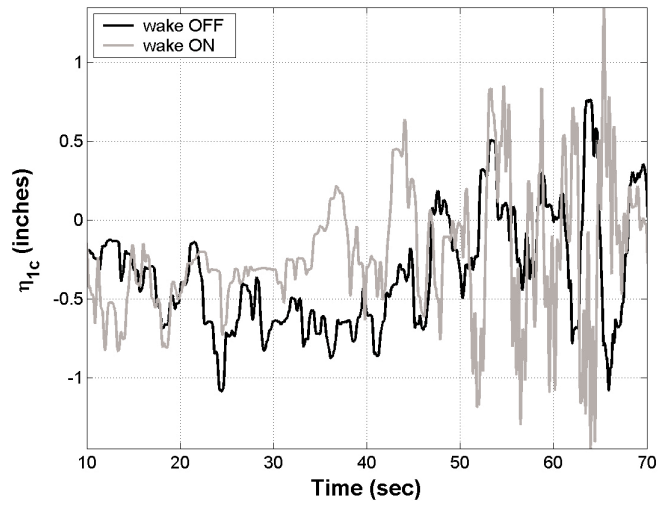


Figure 11. Pilot lateral cyclic activity with and without 0° airwake.

The mission of interest in this work is the recovery of a maritime helicopter to the deck of a single-spot frigate. There are numerous ways to accomplish this depending on the environmental conditions encountered but, as noted earlier, we have confined our interest to the standard UK Royal Navy practice for a port side forward facing recovery. Following this technique the aircraft is flown along a 3° descent and brought to a stabilised hover on the port side of the ship. The pilot then manoeuvres sideways over the deck to a hover position above the landing spot and performs a vertical landing[3]. Previous studies[17,37] have identified the sidestep/landing phase as being the most demanding in terms of pilot workload, so the simulated mission was reduced to just two MTEs; sidestep and vertical landing. However, the sidestep task was found to be unrepresentatively difficult in the simulator, due to the restricted Field of View (FoV), particularly in the horizontal where the FoV is 135°. It was therefore necessary to relax the requirements of the sidestep MTE in order to allow an oblique translation, which afforded the pilot an improved view of the flight deck. This oblique translation is shown in Fig. 12; the slightly irregular nature of the line of flight is because this is an actual path flown by the test pilot in the simulator under the influence of an airwake.

Desired and adequate performance criteria are normally defined for each MTE. In this case however the pilot was instructed to fly the manoeuvres at levels of precision and aggression employed in typical service operations. The intention being that the results of this trial should inform the definition of suitable performance criteria for future trials. The only performance constraint placed on the pilot was to touchdown within the 3·5m (11·5ft) radius circle painted on the flight deck of the frigate visual model at an appropriate descent rate.

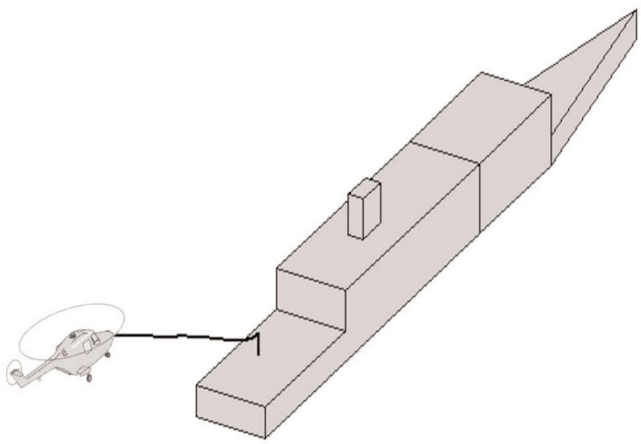


Figure 12. The simulated oblique translation/vertical landing.

Variations in relative wind speed were achieved by scaling the airwake velocity components by an appropriate factor. The CFD simulations were originally carried out using a free-stream wind velocity of approximately 40kt. Therefore, the scaling factor required to give a relative wind speed of 30kt was 0·75, 50kt was 1·25 and so on. Variations in the relative wind direction were achieved by loading a different airwake data file.

The simulator trials were conducted in the same style as an at-sea first-of-class flight trial, starting initially with a very benign test point and gradually working up to more difficult conditions in a progressive manner. After each landing the test team would analyse the data and pilot comments from that run and make a collective decision to either progress to the next wind speed condition for that wind direction or establish a boundary of the SHOL envelope. If it was considered that a limit had been reached then the airwake data file for the next wind direction would be loaded and testing would begin again from a low relative wind speed in the same manner.

4.2 Data collection

The test pilot was asked to subjectively rate his workload using the 10-point Bedford workload ratings scale[38] shown in Fig. 13, which is based on the established Cooper-Harper handling qualities rating system[39]. Two ratings were provided: one for the oblique translation and one for the vertical landing. In the Bedford workload rating system a rating of 1 is assigned to tasks that present the least difficulty. More difficult tasks, that diminish the pilot's spare capacity to perform additional tasks, are awarded increasingly higher ratings. A single workload rating was also given for the complete mission using the Deck Interface Pilot Effort Scale (DIPES). The DIPES scale (Fig. 14) is also used during at-sea testing. We consider the Bedford and DIPES scales to be less well known than the Cooper-Harper and have therefore included them in this paper for completeness. Wind conditions that attain a rating of 3 or less on the DIPES scale are considered acceptable and within the envelope of the SHOL. DIPES ratings of 4 or 5 are considered unacceptable and are outside the boundaries on the SHOL diagram. As well as giving detailed comments the pilot also provided one or more suffixes to the DIPES rating to describe the cause of the increased workload during each task. The pilot who performed the simulation trials was a highly experienced former Royal Navy test pilot who has been involved in numerous FOCFTs, but when giving a rating he was asked to consider the capabilities of an 'average' fleet pilot, this is entirely consistent with the approach taken during FOCFTs. A video recording of the centre channel of the simulator outside world and an audio log of the pilot's commentary were taken during the trials. Various aircraft parameters including pilot control inceptor activity, flight path, aircraft attitude, and engine and rotor parameters were also captured to enable detailed post-trial analysis.

4.3 Results

Figure 15 shows the pilot workload ratings for the oblique translation and vertical landing MTEs. It is clear from this figure that pilot workload varies considerably with changes in relative wind speed and direction. Areas of particularly high pilot workload are experienced in the Green 30 to Green 60 region with wind strengths of 30 knots or more and for airwakes with strong aft or tail wind components. The increased activity in Green 30° to 60° was due to a combination of increased collective activity to control height over the deck, increased pedal activity to control yaw, and increased difficulty in lateral positioning. For the aft or tail winds

https://doi.org/10.1017/S0001924000001329 Published online by Cambridge University Press

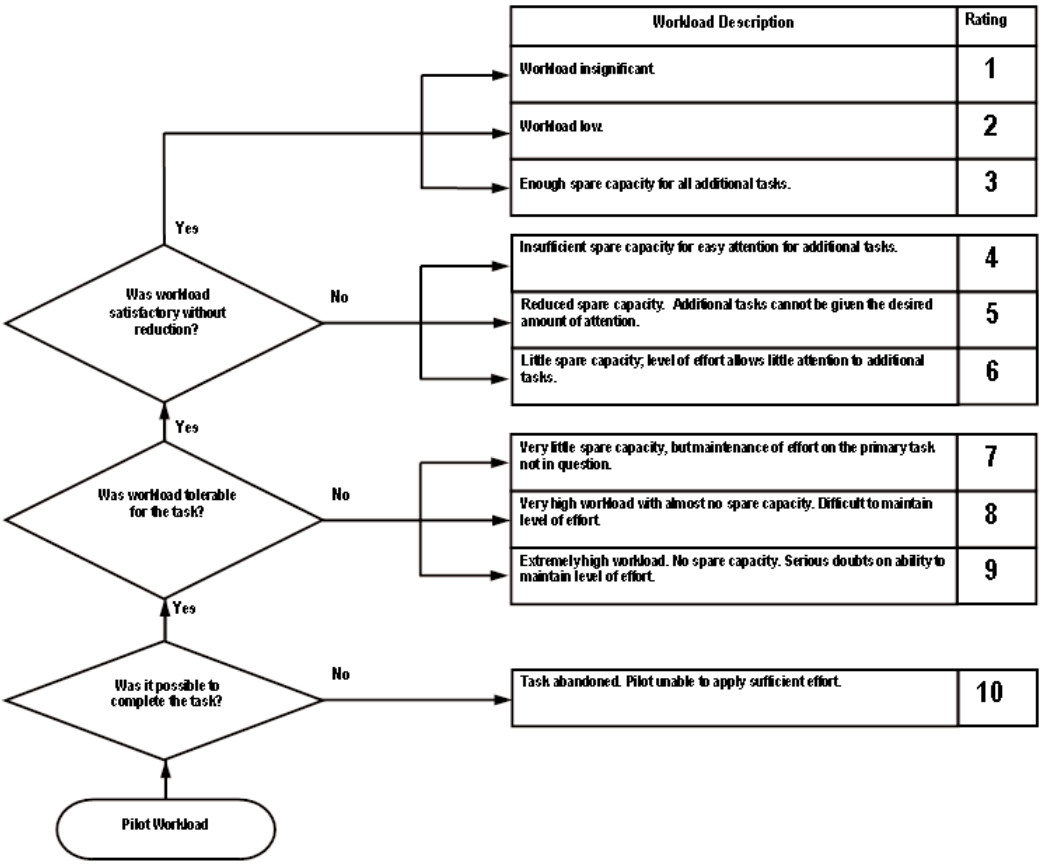


Figure 13. The Bedford workload ratings scale.

most of the workload was associated with yaw control and the aircraft attitude. These high pilot workload ratings suggest a possible need for limits in these areas, to protect the pilot from exposure to high levels of workload during deck landings. Not all the airwake models could be tested due to operational constraints in the simulation laboratory so effort was concentrated on the fore and aft winds; trials with side winds were curtailed so there is little data in this region on which to base the SHOL.

Although subjective pilot workload ratings are an important parameter in defining the SHOL limits, other factors such as the ability of the pilot to perform the recovery consistently in a safe and accurate manner without exceeding aircraft control margins are also important. After subsequent post-trials analysis of the data and pilot commentary it became very clear that the pilot was taking all of these aspects into consideration and this is reflected in the DIPES ratings that were awarded at each wind condition.

The SHOL in Fig. 16 has been derived by drawing an envelope encompassing all of the acceptable DIPES ratings, but excludes any unacceptable ratings. The shaded regions represent areas where the SHOL envelope could possibly be expanded had a wider range of wind conditions been investigated. The dotted line is an estimate of the SHOL limits in the side wind region, based on the maximum side wind component investigated during typical FOCFTs[40]. For relative winds between Red 15° and Green 15° no handling limits were identified up to 50kt, which was the maximum tested as this was considered to be a reasonable WOD limit for operational service.

A comparison of Figs 15 and 16 reveals areas of agreement where the SHOL is dictated entirely by pilot workload considerations. The cause of high pilot workload and DIPES ratings could often be attributed to increased workload in one of the four pilot control channels: lateral cyclic, longitudinal (fore/aft) cyclic, collective or rudder pedals, or a combination of control channels. Figure 17 shows the power spectral density of the pilot's control inputs for just the lateral cyclic axis for a Green 60° wind with relative wind speeds of 30kt (DIPES2), 40kt (DIPES3) and 50kt (DIPES4). These power spectra show the amount of control 'energy' applied by the pilot over the typical range of closed-loop control frequencies. The peaks in the lateral cyclic control power spectra in Fig. 17 can be directly attributed, through pilot comments and recorded data, to increased workload caused by difficulty in lateral positioning accuracy when attempting to perform a vertical landing, and roll attitude transients experienced when crossing the port edge of the deck during the translation manoeuvre. Both of these effects are due to the introduction of the airwake. In other areas where limits exist in regions of low pilot workload, the limits are caused by other factors such as helicopter control margin limits on the Red side of the SHOL, and excessive nose-up hover attitude requirements in the aft portion of the SHOL.

The outcome of this study and the response of the test pilot were very encouraging, particularly given the simplicity of the ship geometry, the steady airwake and the lack of ship motion. The test pilot confirmed that the translation and landing manoeuvres carried out in the simulation environment were generally realistic, but

https://doi.org/10.1017/S0001924000001329 Published online by Cambridge University Press

noticeably lacked the unsteady buffeting experienced during at-sea trials. It is anticipated that inclusion of the unsteady airwakes would capture this experience and would also reduce the SHOL envelope from this initial prediction for the SFS2. Similarly, the inclusion of the interaction of the rotor downwash with the structure of the ship, and including a moving ship may also reduce the envelope towards a more realistic SHOL. However, in the currently predicted SHOL, the general trends were clearly identified and were as expected when compared to known SHOL envelopes. The methodology having now been established will form the foundation for further research in this area.

5.0 CONCLUSIONS AND FURTHER WORK

CFD calculations for the airwakes produced by the simplified frigate shapes, SFS1 and SFS2, have been carried out and compared to wind tunnel data giving satisfactory to good agreement. The agreement was dependent upon a good quality adapted grid. Extensive steady-state calculations have produced a database of airwakes for a range of relative wind directions.

The steady-state airwake database for the SFS2 has been successfully implemented in the flight simulation environment, driven by FLIGHTLAB software. Piloted trials over a range of wind directions and speeds have been carried out with a Lynx-like generic helicopter model, and evaluated using pilot workload and control limit ratings, together with data acquisition and analysis. Using the ratings given by the test pilot, a steady-state SHOL was plotted for the SFS2/generic helicopter combination. The lack of unsteadiness in the airwake data, together with the simplified ship geometry on a stationary sea, resulted in lower workloads than normally experienced, but trends due to wind strength and direction were correctly predicted. Helicopter control limits were also well represented.

The HELIFIGHT lateral FoV is ±67·5°; this caused difficulties during the lateral sidestep tasks. In a typical maritime rotorcraft the pilot would have the benefit of side windows. Although the FoV is currently a physical limitation of the simulator, it is recognised that future work will need to address this in order to allow a more representative deck landing task to be performed.

Continuing work will next implement a test-case unsteady SFS2 airwake into the flight simulator to compare the pilot workload with the corresponding steady results. The outcome of the test case will indicate whether extensive (and expensive) unsteady simulations are justified. At present, the authors and the test pilot believe that unsteadiness is likely to result in more realistic simulations that present the pilot with time-dependent disturbance-rejection tasks, making it more difficult to maintain station close to the ship. The inclusion of the helicopter downwash in a range of spatial locations, together with more realistic frigate geometries and ship motion, are other areas where the CFD database can be expanded for future SHOL trials in the simulation environment.

ACKNOWLEDGEMENTS

This study was funded by an EPSRC Doctoral Training Award for the first author. The authors wish to acknowledge the assistance of Binoy Manimala, Ben Lawrence and Helen Baker of the Flight Science and Technology Research Group at Liverpool. We also

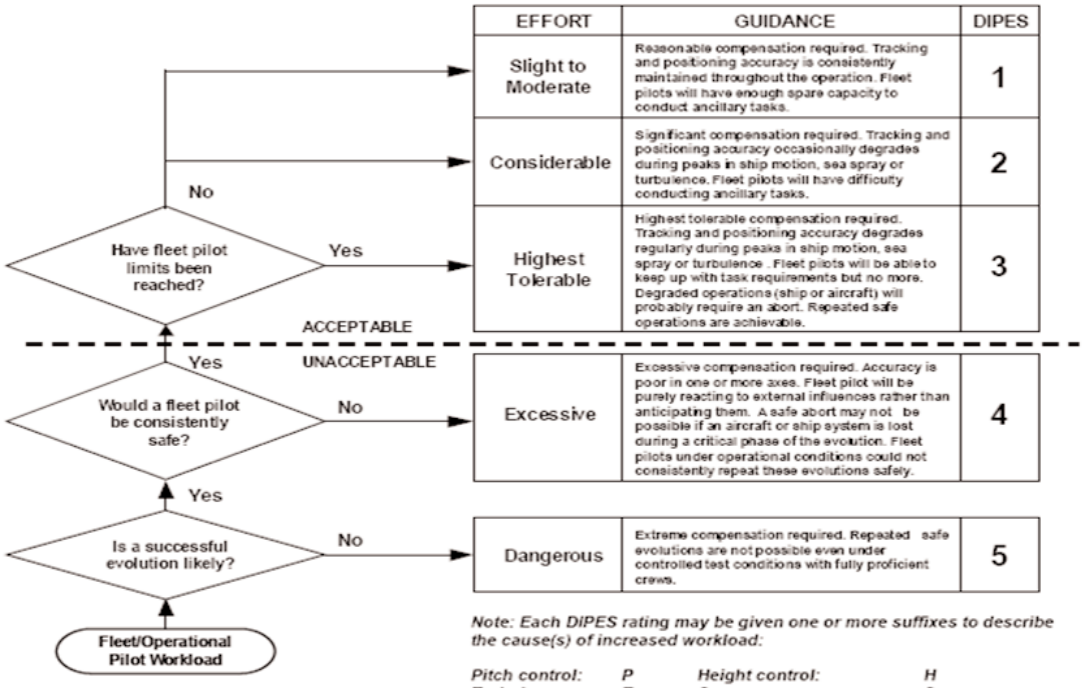


Figure 14. The Deck Interface Pilot Effort Scale (DIPES).

https://doi.org/10.1017/S0001924000001329 Published online by Cambridge University Press

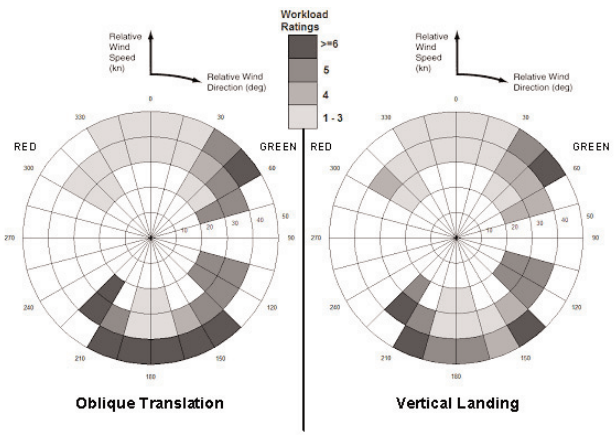


Figure 15. Pilot workload ratings for oblique translation and vertical landing MTEs.

wish to thank the test pilot, Mr Andy Berryman, for his professionalism and guidance. The FLIGHTLAB helicopter model was based on a version of the Lynx provided by QinetiQ. The experimental validation data provided by Dr Steve Zan of NRC Canada is greatly appreciated.

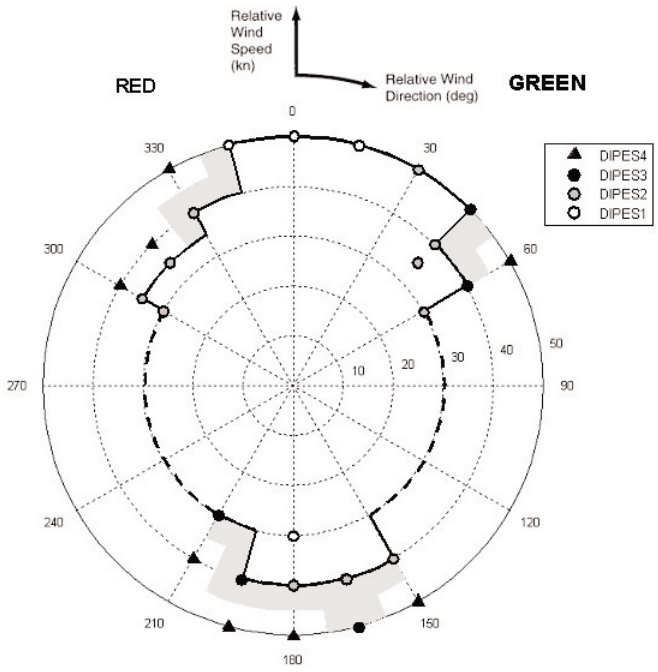


Figure 16. The Liverpool generic model / simple frigate shape 2 Ship-Helicopter Operating Limits chart (SHOL).

REFERENCES

1. HEALEY, J.V. Establishing a database for flight in the wakes of structures, *J Aircr*, 1992, **29,** (4), pp 559-564.
2. ZAN, S.J. and SYMS, G.F. Numerical prediction of rotor loads in an experimentally-determined ship airwake, National Research Council of Canada, Ottawa, April 1995, (Report No LTR-AA-15).
3. LUMSDEN, B. and PADFIELD, G.D. Challenges at the helicopter-ship dynamic interface, Military Aerospace Technologies — Fitec '98, Bury St Edmunds, England. 1998, pp 89-122, (IMechE Conference Transactions).
4. REDDY, K.R., TOFFOLETTO, R. and JONES, K.R.W. Numerical simulation of ship airwake, *Computers & Fluids,* 2000, **29,** (4), pp 451-465.
5. POLSKY, S.A. and BRUNER, C.W.S. Time-accurate computational simulations of an LHA ship airwake, 18th AIAA Applied Aerodynamics Conference, Denver, CO, USA, 14-17 August 2000, (AIAA-2000-4126).
6. SHARMA, A. and LONG, L.N. Airwake simulations on an LPD 17 ship, 15th AIAA Computational Fluid Dynamics Conference, Anaheim, CA, USA, 11-14 June 2001, (AIAA-2001-2589).

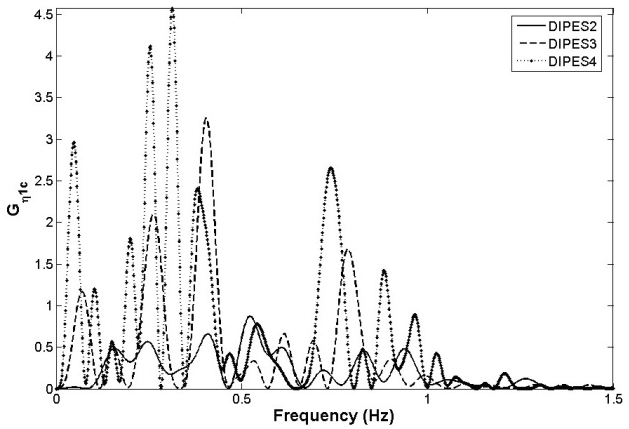


Figure 17. Lateral cyclic control power spectra for Green 60°.

7. ZAN, S.J. Surface flow topology for a simple frigate shape, *Canadian Aero and Space J,* 2001, **47,** (1), pp 33-43.
8. BOGSTAD, M.C., HABASHI, W.G., AKEL, I. and AIT-ALI-YABIA, D. Computational-fluid-dynamics based advanced ship-airwake database for helicopter flight Simulators, *J Aircr,* 2002, **39,** (5), pp 830-838.
9. POLSKY, S.A. A computational study of unsteady ship airwake, 40th AIAA Aerospace Sciences Meeting & Exhibit, Reno, Nevada, USA, 14-17 January 2002, (AIAA-2002-1022).
10. ZAN, S.J. Experimental determination of rotor thrust in a ship airwake, *J American Heli Soc,* 2002, **47,** (2), pp 100-108.
11. SYMS, G.F. Numerical simulation of frigate airwakes, *Int J Computational Fluid Dynamics*, 2004, **18,** (2), pp 199-207.
12. LEE, R.G. and ZAN, S. Wind tunnel testing of a helicopter fuselage and rotor in a ship airwake, *J American Heli Soc,* 2005, **50,** (4), pp 326-337.
13. HEALEY, J.V. The prospects for simulating the helicopter-ship interface, *Naval Engineers J*, 1987, **99,** (2), pp 45-63.
14. O'REILLY, P.J.F. Aircraft/deck interface dynamics for destroyers, *Marine Technology,* 1987, **24,** (1), pp 15-25.
15. ARNEY, A.M., BLACKWELL, J. and FEIK, R.A. Modelling the helicopter/ship dynamic interface, National Conference Publication — Institution of Engineers, Australia, 1989, **89,** (pt 14), p 23.
16. BLACKWELL, J., ARNEY, A.M., GILBERT, N.E. and TRUONG, T.T. Modelling the helicopter/ship dynamic Interface for the Seahawk/FFG-7. Proceedings of the 5th Australian Aeronautical Conference, Melbourne, Australia, 13-15 September 1993, **2,** (2), pp 277-284. (National Conference Publication — Institution of Engineers, Australia).
17. TATE, S.J. and PADFIELD, G.D. Simulating flying qualities at the helicopter/ship dynamic interface, Proceedings of the 50th Annual Forum of the American Helicopter Society, Washington, DC, USA, 11-13 May 1994.
18. ROSCOE, M.F. and Thompson, J.H. JSHIP's dynamic interface modeling and simulation system: A simulation of the UH-60A Helicopter/LHA shipboard environment task. Proceedings of the 59th Annual Forum of the American Helicopter Society, Phoenix, Arizona, USA, 6-8 May 2003.
19. MIN, Z., CHANG, C., SIANG, S.C., YONG, L.N., JACQUELINE, S.Z.Q. and ADRIAN, W.T.B. Analytical approach to helicopter-ship certification, Proceedings of the 60th Annual Forum of the American Helicopter Society, Baltimore, MD, USA, 7-10 June, 2004, **1**, pp 257-268.
20. CARICO, D., MCCALLUM, K.E. and HIGMAN, J. Dynamic interface flight test and simulation limitations, Eleventh European Rotorcraft Forum, London, England. 1985, pp 100-1.

https://doi.org/10.1017/S0001924000001329 Published online by Cambridge University Press

21. PADFIELD, G.D. Simulating flying qualities at the helicopter/ship dynamic interface. Proceedings of the 50th Annual Forum of the American Helicopter Society, Washington, DC, USA, 11-13 May, 1994, **2,** (2), pp 883-904. (Annual Forum Proceedings — American Helicopter Society).
22. REDDY, K.R. and TRUONG, T. Effect of ship airwake interference on helicopter trim and control positions, Proceedings of the 12th Australasian Fluid Mechanics Conference, Sydney, Australia, 1995. pp 691-5.
23. BRADLEY, R. and TURNER, G. Simulation of the human pilot applied at the helicopter/ship dynamic interface, Proceedings of the 55th Annual Forum of the American Helicopter Society, Montreal, Canada, 1999, **1,** pp 677-688.
24. PADFIELD, G.D. and TURNER, G.P. Helicopter encounters with aircraft vortex wakes, *Aeronaut J,* 2001, **105,** (1043), pp 1-8.
25. TURNER, G.P., PADFIELD, G.D. and HARRIS, M. Encounters with aircraft vortex wakes: the impact on helicopter handling qualities, *J Aircr*, 2002, **39,** (5), pp 839-849.
26. LEE, D., HORN, J.F., SEZER-UZOL, N. and LONG, L.N. Simulation of pilot control activity during helicopter shipboard landing, AIAA Atmospheric Flight Mechanics Conference and Exhibit, Austin, Texas, USA, 11-14 August 2003, (AIAA-2003-5306).
27. ADVANI, S.K. Dynamic interface modelling and simulation — A unique challenge, RAeS Conference on Helicopter Flight Simulation, London, UK, November 2001.
28. *Flight International* article: Apache finds its sea legs, http://www.flightinternational.com/Articles/2004/07/20/184525/Apache+finds+its+sea+legs.html.
29. CHENEY, B.T. and ZAN, S.J. CFD code validation and flow topology for the technical co-operation program AER-TP2 simple frigate shape, National Research Council of Canada, Institute for Aerospace Research, April, 1999, (Report No NRC-IAR-LTR-A-035).
30. SCHEWE, G. Investigation of the aerodynamic forces on bluff bodies at high Reynold's numbers, European Space Agency, June 1985, (Report No ESA-TT-914).
31. LEE, R.G. SFS2 mean flows & intensities, Unpublished data provided by the National Research Council of Canada, 2003.
32. PADFIELD, G.D. and WHITE, M.D. Flight simulation in academia – HELIFLIGHT in its first year of operation at the University of Liverpool, *Aeronaut J,* 2003, **107,** (1075), pp 529-538.
33. WHITE, M.D. and PADFIELD, G.D. Flight simulation in academia – progress with HELIFLIGHT at the University of Liverpool, RAeS Conference 'Flight Simulation 1929-2029: A Centennial Perspective', London, UK, 26-27 May 2004.
34. PADFIELD, G.D. *Helicopter Flight Dynamics: The Theory and Application of Flying Qualities and Simulation Modelling,* Oxford, Blackwell Science, 1996.
35. MCCALLUM, A.T., PADFIELD, G.D. and SIMPSON, A. Current studies in rotorcraft simulation validation at DRA Bedford, The Royal Aeronautical Society Conference on Rotorcraft Simulation, London, May 1994.
36. PADFIELD, G.D. The making of helicopter flying qualities: a requirements perspective, *Aeronaut J,* 1998, **102,** (1018), pp 409-437.
37. PADFIELD, G.D. and WILKINSON, C.H. Handling qualities criteria for maritime helicopter operations, Proceedings of the 53rd Annual Forum of the American Helicopter Society, Virginia Beach, VA, USA, 29 April – 1 May 1997, **2,** (2), pp 1425-1440.
38. ROSCOE, A.H. and ELLIS, G.A. A subjective rating scale for assessing pilot workload in flight, RAE Technical Report, March, 1990, (Report No 90019).
39. COOPER, G.E. and HARPER, R.P. The use of pilot rating in the evaluation of aircraft handling qualities, NASA Technical Note, Washington, DC, April, 1969, (Report No TN-D-5153).
40. FINDLAY, B.A. United Kingdom approach to delivering military ship helicopter operating limits, Proceedings of Aircraft/Ship Operations, Seville, Spain, 1991, pp 20-23. (AGARD-CP-509).

https://doi.org/10.1017/S0001924000001329 Published online by Cambridge University Press